Cancer Research

Proinflammatory CXCL12–CXCR4/CXCR7 Signaling Axis Drives Myc-Induced Prostate Cancer in Obese Mice

Achinto Saha[1], Songyeon Ahn[1], Jorge Blando[1], Fei Su[2], Mikhail G. Kolonin[2], and John DiGiovanni[1]

Abstract

Obesity is a prognostic risk factor in the progression of prostate cancer; however, the molecular mechanisms involved are unclear. In this study, we provide preclinical proof of concept for the role of a proinflammatory CXCL12–CXCR4/CXCR7 signaling axis in an obesity-driven mouse model of myc-induced prostate cancer. Analysis of the stromal vascular fraction from periprostatic white adipose tissue from obese HiMyc mice at 6 months of age revealed a dramatic increase in mRNAs encoding various chemokines, cytokines, growth factors, and angiogenesis mediators, with CXCL12 among the most significantly upregulated genes. Immunofluorescence staining of ventral prostate tissue from obese HiMyc mice revealed high levels of CXCL12 in the stromal compartment as well as high staining for CXCR4 and CXCR7 in the epithelial compartment of tumors. Prostate cancer cell lines derived from HiMyc tumors (HMVP2 and derivative cell lines) displayed increased protein expression of both CXCR4 and CXCR7 compared with protein lysates from a nontumorigenic prostate epithelial cell line (NMVP cells). CXCL12 treatment stimulated migration and invasion of HMVP2 cells but not NMVP cells. These effects of CXCL12 on HMVP2 cells were inhibited by the CXCR4 antagonist AMD3100 as well as knockdown of either CXCR4 or CXCR7. CXCL12 treatment also produced rapid activation of STAT3, NFκB, and MAPK signaling in HMVP2 cells, which was again attenuated by either AMD3100 or knockdown of CXCR4 or CXCR7. Collectively, these data suggest that CXCL12 secreted by stromal cells activates invasiveness of prostate cancer cells and may play a role in driving tumor progression in obesity. Targeting the CXCL12–CXCR4/CXCR7 axis could lead to novel approaches for offsetting the effects of obesity on prostate cancer progression. *Cancer Res; 77(18); 5158–68. ©2017 AACR.*

Introduction

Data associating obesity and prostate cancer risk have been inconclusive (1, 2); however, a number of studies have shown increased risk of biochemical failure and metastasis, as well as poorer survival among obese prostate cancer patients with androgen-dependent tumors, especially those who experienced rapid weight gain (3). Men with low-volume prostate cancer have a lower BMI, less body fat, and a smaller waist-to-hip ratio than men with high-volume prostate cancer, which agrees with other reported findings (4, 5). Fat is the most energy-dense dietary component and has been the focus of most prostate cancer dietary epidemiologic investigations. High consumption of energy and fat, especially saturated fat (6, 7), is associated with advanced stage prostate cancer and mortality (6, 8). As the prevalence of obesity increases (9), a clearer understanding of the underlying mechanism(s) and its link with cancer aggressiveness are urgently needed to develop new strategies for reducing prostate cancer–related morbidity and mortality.

Abdominal obesity, resulting from overgrowth of visceral white adipose tissue (WAT), has been specifically linked with progression of prostate cancer (10, 11). The state of chronic inflammation ensuing as a result of pathologic WAT overgrowth has been proposed to play a role in linking obesity and cancer (12, 13). WAT is a potent endocrine organ (14), comprised of mature adipocytes, together with other cell types known specifically as the stromal vascular fraction (SVF). The SVF consists of mesenchymal adipocyte progenitors termed adipose stromal cells (ASC), monocytes, macrophages, and other infiltrating leukocytes (13, 15). These cells contribute to the production of adipokines, among which IGF-1, IL6, TNFα, leptin, adiponectin, and steroid hormones are implicated in cancer (16, 17). Specifically, periprostatic WAT (ppWAT), which is expanded in obesity, is believed to play a significant role in promoting prostate cancer progression (18, 19).

Recent studies have suggested an important role of chemokines in prostate cancer progression (20, 21). Chemokines are small chemotactic cytokines involved in a variety of developmental processes in addition to their function in recruitment and activation of leukocytes and directed migration of invasive cancer cells (22–24). One of the chemokines promoting cancer progression is CXCL12, also known as stromal-derived factor-1 (SDF-1). CXCL12 is a potent chemoattractant for hematopoietic cells (25)

[1]Division of Pharmacology and Toxicology, Dell Pediatric Research Institute, The University of Texas at Austin, Austin, Texas. [2]The Brown Foundation Institute of Molecular Medicine for the Prevention of Disease, The University of Texas Health Sciences Center at Houston, Houston, Texas.

Note: Supplementary data for this article are available at Cancer Research Online (http://cancerres.aacrjournals.org/).

Current address for J. Blando: Immunopathology Laboratory Immunotherapy Platform, The University of Texas MD Anderson Cancer Center, Houston, TX.

Corresponding Author: John DiGiovanni, The University of Texas at Austin, 1400 Barbara Jordan Boulevard, Austin, TX 78723. Phone: 512-495-4726; Fax: 512-495-4945; E-mail: john.digiovanni@austin.utexas.edu

doi: 10.1158/0008-5472.CAN-17-0284

and activates signaling events through two different receptors, CXCR4 and CXCR7 (24). Binding of CXCL12 to CXCR4 induces trimeric G protein signaling, leading to activation of the Src, PI3K/AKT, ERK, and JNK pathways, contributing to protease production and cellular migration and invasion (22, 26). CXCR4 has been shown to be a key receptor in mediating the metastasis of multiple types of tumors (27). The role of CXCL12–CXCR4 axis in cancer cell migration, invasion, and metastasis has been demonstrated (28–31). AMD3100, a CXCR4 inhibitor, sensitizes prostate cancer to chemotherapy (32); however, the main source of CXCL12 and its contribution to obesity-associated cancer progression has not been investigated.

We previously reported the effect of dietary energy balance manipulation on cancer development and progression in HiMyc mice (33), a spontaneous genetic prostate cancer model. The HiMyc mouse tumors share molecular and histopathologic features with human prostate tumors (34). c-Myc is overexpressed in many cancers, including prostate cancer (35, 36). The *MYC* locus (8q24) is amplified in patients (37), which correlates with high histologic grade scores and a worse prognosis (38). Upregulation of nuclear c-MYC protein expression is a highly prevalent and early change in human tumors, which suggests that it drives cancer initiation (39). In the HiMyc model, overexpression of c-Myc in the prostate is directed via the ARR_2Pb probasin promoter (34). Prostatic epithelial expression of c-Myc in the dorsolateral prostate, ventral prostate (VP), and anterior prostate (AP) lobes results in complete penetrance of PIN as early as 2 to 4 weeks of age, which progressed to locally invasive adenocarcinomas within 6 to 12 months of age (34). Although the HiMyc model is not metastatic, it is advantageous for studying the obesity–cancer relationship because there is sufficient time to establish diet-induced obesity (DIO) and study disease progression.

We recently reported the effect of dietary energy balance manipulation across the spectrum of calorie restriction (CR) to DIO on prostate cancer development and progression in HiMyc mice (33). Male HiMyc mice were placed on three dietary regimens, 30% CR, a modified AIN76A with 10 kcal% fat, and a DIO regimen (60 kcal% fat), resulting in cohorts of lean, overweight, and obese animals. All diet groups had an approximately similar incidence of hyperplasia and low-grade PIN in the VP at 3 and 6 months of age. However, 30% CR significantly reduced the incidence of *in situ* adenocarcinoma at 3 months compared with the DIO group and at 6 months compared with both the overweight control and DIO groups. The DIO regimen significantly increased the incidence of adenocarcinoma with aggressive stromal invasion, as compared with the overweight group (96% vs. 65%, respectively, $P = 0.02$) at the 6-month time point. In addition, at both 3 and 6 months, only *in situ* carcinomas were observed in mice maintained on the 30% CR diet. Expression of both growth factor and inflammatory genes was significantly increased in prostate tissue obtained from obese HiMyc mice compared with mice on both the control and CR diets (33).

Here, we provide evidence that CXCL12 signaling through CXCR4 and CXCR7 mediates obesity-induced prostate cancer progression in HiMyc mice (33). We show that DIO leads to increased expression of CXCL12 from the SVF of ppWAT and demonstrate that CXCL12 is expressed by ASCs. CXCL12 selectively stimulated migration and invasion of murine prostate cancer cells derived from HiMyc mice (HMVP2 cells; ref. 40) compared with nontumorigenic prostate epithelial cells derived from FVB/N mice. CXCL12 also induced several important oncogenic signaling pathways, including STAT3, NFκB, and MAPK in prostate cancer cells. The migration, invasion, and activation of signaling events were abrogated by inhibition (either pharmacologically or genetically) of CXCR4 or CXCR7, indicating that CXCL12 functions through these receptors in mouse prostate cancer cells. Collectively, these data demonstrate an important role of ASC-derived CXCL12, in obesity-driven prostate cancer progression.

Materials and Methods

Cell culture

The murine prostate cell lines NMVP, HMVP1, HMVP2, HMVP2A1, and HMVP2A2 were generated in our laboratory from the mouse ventral prostate in 2012 as described previously (40), and we periodically check for the expression of prostate epithelial cell markers. No futher authentication was performed. NMVP cells were cultured in DMEM/F12 (Lonza) medium containing 10% FBS, bovine pituitary extract (28 mg/mL; Hammond Cell Tech), EGF (10 ng/mL; Sigma-Aldrich), insulin (8 mg/mL; Sigma-Aldrich), and transferrin (5 mg/mL; Sigma-Aldrich). All other cell lines were cultured in RPMI1640 (Life Technologies) medium containing 10% FBS (Life Technologies). Cell lines were regularly (every 2 months) evaluated for mycoplasma by PCR with commercially available PCR Mycoplasma Detection Kit (Applied Biological Materials, Inc.). All experiments were performed within 1 month after thawing the cells. All cells were maintained in 95% air and 5% CO_2 at 37°C.

Isolation of SVF

HiMyc mice (34) were obtained from the NIH MMRRC on an FVB/N genetic background and bred in-house for the current experiments. Diets were purchased from Research Diets, Inc. For all the studies, mice were housed in suspended polycarbonate cages on autoclaved hardwood bedding at room temperatures of 20°C to 22°C, relative humidity of 60% to 70%, and 14/10-hour light/dark cycle. All animal studies have been conducted in accordance with an approved Institutional (The Univerity of Texas at Austin, Austin, TX) Animal Care and Use Committee protocol. Mice were placed on AIN76A semipurified diet at 4 to 5 weeks of age for a 1-week equilibration period and then randomized into the following dietary groups for the duration of the study: (i) 30% CR diet, (ii) control diet (continued on the modified AIN76A diet, 10 kcal% fat), fed *ad libitum*; and (iii) DIO diet (60 kcal% fat), fed *ad libitum* as described previously (33). Groups of mice were terminated by CO_2 asphyxiation at 6 months of age, and ppWAT were collected and immersed in DMEM (Life Technologies) media. The pooled ($n = 5$) fat tissues were minced into fine pieces and resuspended in equal volume of digestion solution containing 0.5 mg/mL collagenase type I (Sigma-Aldrich) and 25 U/mL dispase (BD) in PBS. The resulting mixture was incubated on water bath at 37°C for 1 hour by shaking every 10 minutes. Then, the samples were centrifuged at 300 × *g* for 5 minutes, and the supernatant including the upper white layer (adipocytes) were aspirated and the cell pellets were resuspended in DMEM containing 5% FBS and 2 mmol/L EDTA (Sigma-Aldrich) and filtered through 100-μm nylon cell strainer followed by rinsing the filter with additional DMEM solution. The cell suspensions were centrifuged at 300 × *g* for 10 minutes, and the pellets were resuspended in PBS with 2 mmol/L EDTA.

Finally, the cell suspensions were centrifuged at 300 × *g* for 10 minutes to isolate the SVF.

qRT-PCR

Total RNA was isolated from the SVF by using Qiagen RNeasy Mini Kit (Qiagen) according to the manufacturer's protocol and subjected to reverse transcription as described previously (33). mRNA levels of genes were quantitatively determined by qRT-PCR using the Viia7 Real Time PCR System (Applied Biosystems) with SYBR Green Master Mix (Qiagen). The relative abundance of the mRNA was normalized against GAPDH mRNA for quantitative evaluation.

Immunofluorescence and immunocytochemical analyses

Immunofluorescence (IF) analyses were performed on formalin-fixed, paraffin-embedded prostate tissue sections, and immunocytochemical (ICC) analyses were performed on cultured HMVP2 cells as described previously (40, 41). Briefly, tissue sections were deparaffinized with serial incubation and washing in xylene, 100%–70% ethanol and water followed by antigen unmasking with citrate buffer. The samples were then blocked for 1 hour at room temperature and incubated with primary antibodies [Perilipin (9349) from Cell Signaling Technology, CD3 (550275) from BD Pharmingen, RM0029-11H3 (ab56297), CXCR7 (ab72100) from Abcam, CXCL12 (sc-28876) from Santa Cruz Biotechnology, CXCR4 (MAB21651) from R&D Systems and αSMA (C6198) from Sigma] overnight at 4°C. Proteins were detected with fluorochrome-conjugated secondary antibodies and visualized using an Olympus BX60 fluorescence microscope.

Migration assay

The migration of cells was measured by a widely used wound healing or scratch assay (42). In brief, cells were seeded in 12-well plates and allowed to grow overnight followed by starvation. Scratch was made in the monolayer confluent cells with sterile 200 μL pipette tips, and the cells were treated with CXCL12 either alone or in combination with AMD3100 (Abcam) for 18 hours. The images were acquired at 0 and 18 hour time points, and migration was calculated from the distance of the closure of the scratch before and after the treatment.

Transwell invasion assay

The invasion of cells was measured by Matrigel transwell invasion chamber (EMD Millipore) assay (43). Cells were seeded into the upper chamber, and the inserts were placed in 24-well plates containing CXCL12, AMD3100, or their combination. Eighteen hours after incubation in a tissue culture incubator, the cells were fixed with 10% formalin solution (Thermo Fisher Scientific), permeabilized with methanol, and stained with Giemsa stain (Sigma-Aldrich). After washing with water, the nonmigrated cells were scraped from the upper chamber with cotton swab, and migrated cells remaining on the bottom surface were counted with an inverted microscope.

Knockdown of CXCR4 and CXCR7

Knockdown of CXCR4 and CXCR7 in HMVP2 cells was performed with pGFP-C-shLenti vector from Origene according to the manufacturer's instructions. Mouse CXCR4 or CXCR7 29mer shRNA constructs (TL500383 and TL515747) with four different sequences were used for both CXCR4 or CXCR7 knockdown and scrambled negative control noneffective shRNA cassette in pGFP-C-shLenti plasmid (TR30021) was used as shRNA control. Cells were infected with lentivirus for 2 days and stable CXCR4 or CXCR7 knockdown cells were generated by puromycin selection. The knockdown efficiency was measured by qRT-PCR and Western blotting.

Western blotting

The following antibodies were used for Western blotting: STAT3 (9139), pSTAT3^{Tyr705} (9145), JNK (9252), pJNK$^{Thr183/185}$ (9251), AKT (9272), pAKT^{Ser473} (4060), ERK1/2 (9102), pERK1/2$^{Thr202/Tyr204}$ (4370), pNFκBp65^{Ser536} (3033) from Cell Signaling Technology; CXCR4 (ab124824), CXCR7 (ab72100) from Abcam; and NFκBp65 (sc-372), β-actin (A5316) from Sigma-Aldrich. After plating, cells were serum starved overnight and treated with CXCL12 for indicated time periods. In some experiments, cells were pretreated with AMD3100 2 hours before the CXCL12 treatment. After incubation, cells were lysed in RIPA buffer. Proteins were separated by SDS-PAGE gel and transferred to nitrocellulose membranes. Levels of phosphorylated and total proteins were measured by Western blot analysis as described previously (33).

Statistical analyses

Statistical analyses were performed using two-tailed Student *t* test or one-way ANOVA followed by Bonferroni multiple comparison tests as applicable. Statistical significance was set at $P < 0.05$.

Results

Recruitment of adipocytes and inflammatory cells to the VP of obese HiMyc mice

HiMyc mice were placed on the three dietary regimens: 30% CR (lean), *ad libitum* 10 kcal% diet (control), and *ad libitum* 60 kcal% diet (DIO). At 6 months of age, VP tissues were subjected to IF analyses. As shown in Fig. 1 (top), staining for perilipin-1, a lipid droplet coat protein, revealed that adipocytes were restricted to ppWAT at the periphery of the VP of lean HiMyc mice. In contrast, adipocytes could be seen infiltrating the VP gland of control HiMyc mice. Notably, in DIO mice, many of the glands in the VP were completely surrounded by adipocytes. We also stained the VP tissues from mice on the three dietary regimens with a CD3 antibody. This revealed infiltration of T lymphocytes (Fig. 1, middle) in the VP of control diet mice, which was even more pronounced in the DIO mice. Similarly, infiltration of macrophages (detected with antibody RM0029-11H3) was dramatically higher in the VP gland of DIO mice compared with the other two diet groups (Fig. 1, bottom). Inflammatory cells were observed in close proximity of the infiltrating adipocytes in the VP of the DIO diet group. Collectively, these results suggest that adipocytes and inflammatory cells recruited into the tumor stroma in obesity might contribute to accelerated prostate cancer progression.

Obesity-induced gene expression changes in the SVF of ppWAT from HiMyc mice

To identify factors secreted by obesity-recruited stroma, we isolated the SVF from the ppWAT of control and obese mice. mRNA was analyzed by qRT-PCR for expression of selected genes previously implicated in the obesity–cancer link (33, 44). As shown in Supplementary Fig. S1A, we observed highly significant

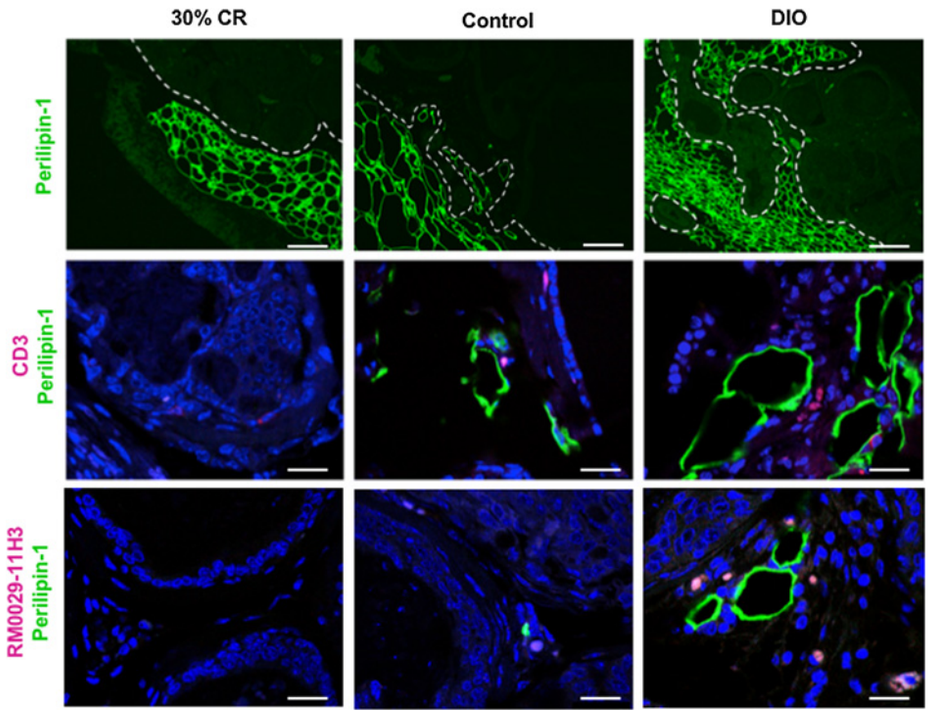

Figure 1.
Recruitment and infiltration of adipocytes and inflammatory cells in the ventral prostate of HiMyc mice as a function of dietary energy balance manipulation. Immunofluorescence analysis of representative prostate tissue sections from HiMyc mice fed on 30% CR, control, or DIO diets with antibodies against perilipin-1, CD3 (T lymphocytes), and RM0029-11H3 (macrophages) with red and green fluorophore-conjugated secondary antibodies. Representative images of tissue sections from 5 mice per group are shown. All tissue sections from each diet group gave similar results. Scale bar, 200 μm (top row) and 25 μm (middle and bottom rows).

upregulation of mRNA levels for IGF-1, IL6, CCL5, IKKα, cyclinD1, cMyc, NFκB1, and RelA (NFκBp65) in SVF from the obese mice. mRNAs for a number of other genes [TGFβ, PDGFα, PDGFβ, HIF-1α, VEGF (A, B, C), IL1α, IL1β, IL7, IL17, IL23, IL23R, and TNFα] were also significantly upregulated in the SVF from from ppWAT of obese HiMyc mice compared with mice on the control diet (Supplementary Fig. S1B and S1C). These data indicate that ASCs and possibly other SVF cells present in ppWAT secrete growth factor and inflammatory mediators that may play an important role in driving prostate cancer progression in obesity.

CXCL12 and its receptors are elevated in VP of obese HiMyc mice

Analysis of mRNA levels demonstrated that CXCL12 expression was highly upregulated in the SVF of ppWAT from obese HiMyc mice (Fig. 2A). Expression of CXCL12 receptors, CXCR4 and CXCR7, was also increased. It has been reported that ASCs secrete large amounts of CXCL12 (45); however, CXCL12 expression in ppWAT has not been investigated. To determine the cellular location of CXCL12 and its receptors in the VP of HiMyc mice, tissue sections from mice on the three different diets were analyzed. As shown in Fig. 2B (top), we detected a higher IF signal for CXCL12 protein in the VP stroma of obese HiMyc mice compared with CR and control diet mice. α-SMA, a myofibroblast marker whose expression is activated in obesity-associated cancer progression (46), was expressed in CXCL12-positive stroma (Fig. 2B, bottom). Expression of CXCR4 and CXCR7, two receptors for CXCL12, was detected primarily in the tumor epithelial compartment in the VP of HiMyc mice (Fig. 2C) and was highest in the VP of obese mice.

We also compared the expression of CXCL12 and and its receptors in cultured immortalized mouse ASCs and HMVP2 cells derived from HiMyc tumors (40). As shown in Supplementary Fig. S1D, the mRNA expression of CXCL12 was significantly higher in the mASCs compared with the HMVP2 cells. In contrast, CXCR4 and CXCR7 mRNA expression was higher in HMVP2 cells than in ASCs. Interestingly, CXCR4 and CXCR7 proteins were expressed in HMVP2 cells as well as in two other more tumorigenic cell lines (HMVP2A1 and HMVP2A2 derived from *in vivo*/*in vitro* passage of HMVP2 cells; ref. 40) to a greater extent than NMVP (nontumorigenic) and HMVP1 (weakly tumorigenic) cells (Fig. 3A). Quantification revealed that HMVP2 cells had approximately 2.5- and 6-fold higher expression of CXCR4 and CXCR7, respectively, compared with NMVP cells, and the two additional prostate cancer cell lines had even higher expression of these receptors (Fig. 3B). Protein expression of CXCR4 and CXCR7 in the more aggressive cancer cells was confirmed by IF (data not shown). These results demonstrate that CXCR4 and CXCR7 expression in prostate cancer epithelium is associated with obesity and cancer aggressiveness.

CXCL12 selectively stimulates migration and invasion of HMVP2 prostate cancer cells

CXCL12 is implicated in chemotaxis of various cell types (reviewed in ref. 24). Therefore, we examined the effect of CXCL12 on migration and invasion of HMVP2 cells compared with NMVP cells that have lower CXCR4 and CXCR7 protein expression. In these experiments, we also compared the effect of IL6, which was also found to be highly upregulated in the SVF from ppWAT of obese HiMyc mice (Supplementary Fig. S1A). CXCL12 had no significant effects on proliferation of any of the cell lines (data not shown). However, CXCL12 stimulated migration of HMVP2 cells (Fig. 4A; Supplementary Fig. S2A) but not NMVP cells (Fig. 4B; Supplementary Fig. S2B). In contrast, IL6 treatment had little or no stimulatory effect on the migration of either HMVP2 or NMVP cells. To further investigate the role of CXCL12 and its receptor, CXCR4, on migration, we pretreated the cells with the CXCR4

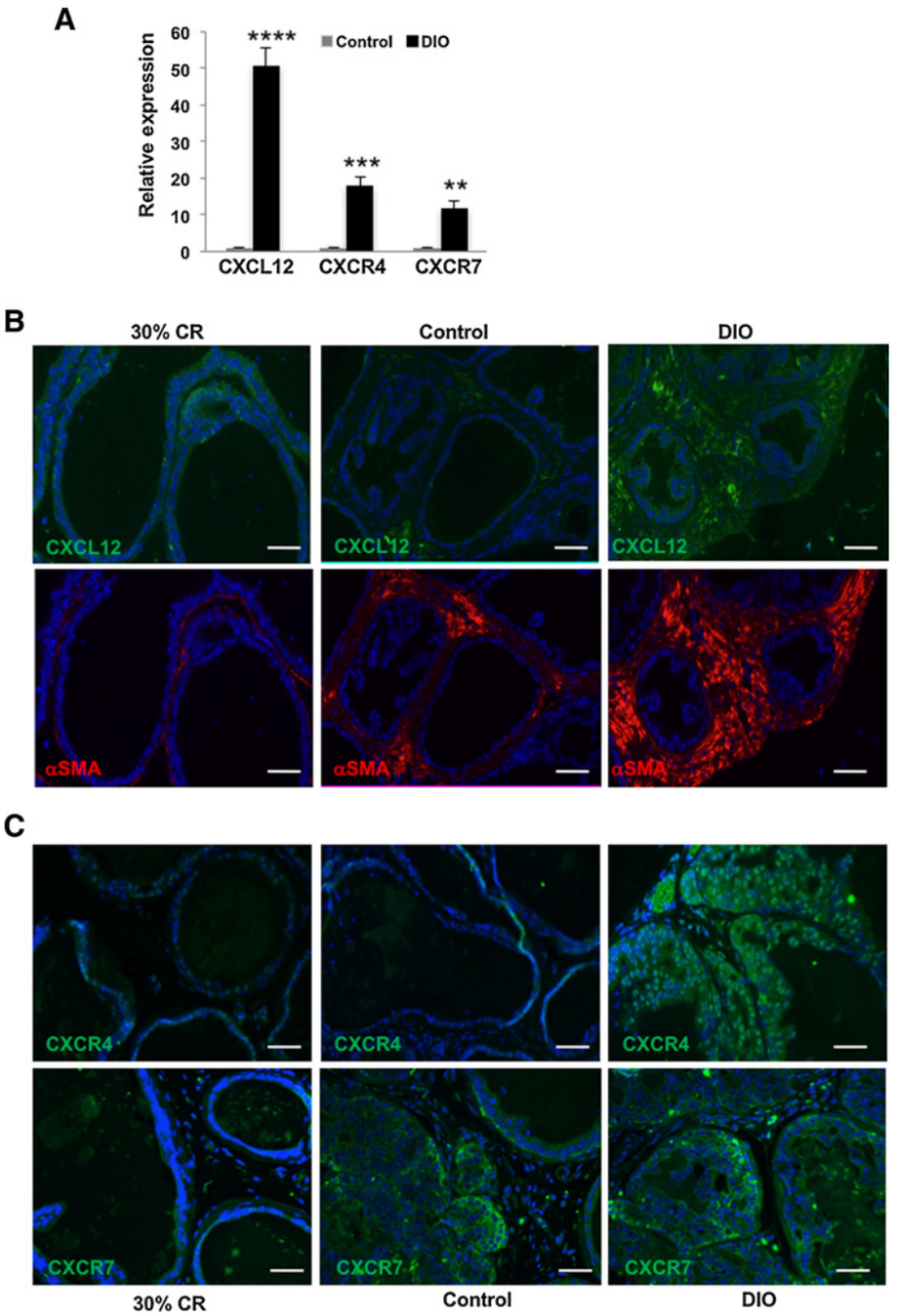

Figure 2.

A, Increased mRNA expression of CXCL12, CXCR4, and CXCR7 in the SVF of obese HiMyc mice. mRNA was isolated from the SVF of adipose tissue surrounding the ventral prostate of HiMyc mice at 6 months of age. Fold change in gene expression in obese mice fed the DIO (60 kcal% fat) diet relative to mice fed the control (10 kcal% fat) diet is shown. Quantitation of fold change of mRNA is presented as mean ± SEM of three independent experiments. Significantly different, **, $P < 0.01$; ***, $P < 0.001$; ****, $P < 0.0001$ (Student *t* test). **B** and **C,** Immunofluorescence analysis of representative prostate tissue sections from age-matched HiMyc mice fed on CR, control, or DIO diet with antibodies against CXCL12, α-SMA, CXCR4, and CXCR7 with red and green fluorophore-conjugated secondary antibodies. Shown are representative images from one mouse of a group of 5 mice. All tissue sections from each diet group gave similar results. Scale bar, 100 μm.

inhibitor, AMD3100 (32), and then stimulated with CXCL12. As shown in Fig. 4, AMD3100 significantly inhibited the CXCL12-induced migration of HMVP2 cells.

As shown in Fig. 4C and Supplementary Fig. S3A, CXCL12 also significantly stimulated invasion of HMVP2 cells but had little effect on the invasion of NMVP cells (Fig. 4D; Supplementary Fig. S3B). Again, IL6 had little or no effect on the invasive properties of HMVP2 cells in this assay. Pretreatment with AMD3100 inhibited CXCL12–induced invasion of HMVP2 cells (Fig. 4). Collectively, these results indicate that CXCL12 stimulates migration and invasion of HMVP2 cells through its receptor, CXCR4. In addition, the data demonstrate a selectivity for the tumor cells compared with nontumorigenic cells based on the level of expression of CXCR4.

Silencing of CXCR4 or CXCR7 attenuates CXCL12-induced migration and invasion

To investigate whether CXCL12-induced migration and invasion of HMVP2 cells is mediated through both CXCR4 and CXCR7, we performed migration and invasion assays with CXCR4

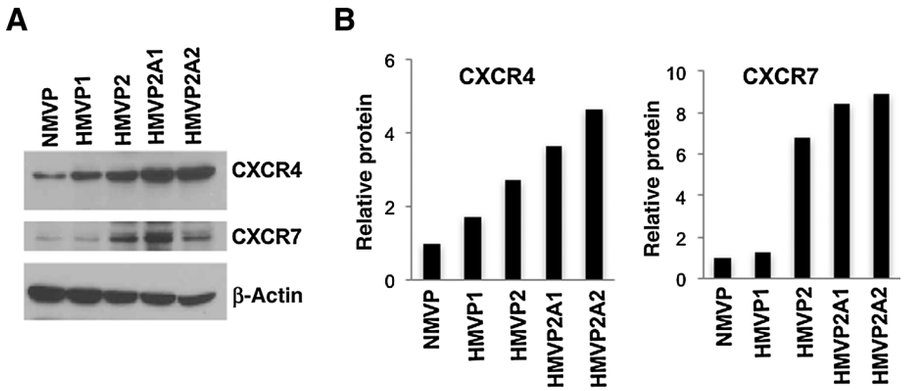

Figure 3.
Increased CXCR4 and CXCR7 protein expression in cancer cell lines. **A,** Protein lysates prepared from cultured cells were subjected to Western blotting. **B,** Relative protein levels were quantitated by densitometry; β-actin was used to control for protein loading. Representative blots of two separate experiments with similar results are shown. Note increased expression in prostate cancer cells compared with normal mouse (NMVP) prostate epithelial cells.

and CXCR7 knockdown cells. We successfully knocked down CXCR4 and CXCR7 with two different targeting sequences, as confirmed by both qRT-PCR (Supplementary Fig. S4A) and Western blotting (Supplementary Fig. S4B and S4C). We performed migration and invasion analysis with CXCR4 and CXCR7-silenced cells in parallel with HMVP2 cells transfected with control nontargeted scrambled shRNA. As shown in Fig. 5A (Supplementary Fig. S5A), treatment with CXCL12 induced significantly less migration in both CXCR4 shRNA-expressing cells compared with the cells with control shRNA. CXCR4 knockdown also decreased the invasiveness of HMVP2 cells, compared with the control shRNA-expressing cells, following CXCL12 treatment (Fig. 5B; Supplementary Fig. S5B). Similarly, CXCR7 silencing also decreased the CXCL12-dependent migration (Fig. 5C; Supplementary Fig. S5C) and invasion (Fig. 5D; Supplementary Fig. S5D) of HMVP2 cells.These results further confirm that CXCL12 induces migration and invasion of HMVP2 cells by signaling thorugh both of its receptors CXCR4 and CXCR7.

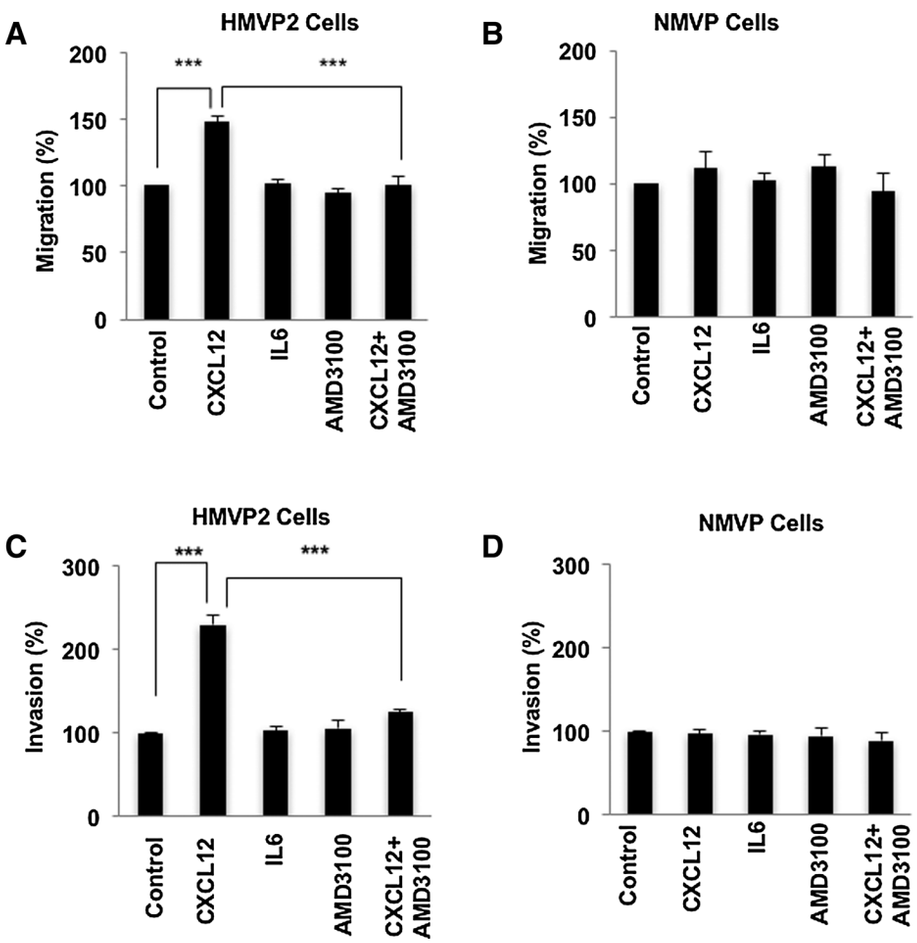

Figure 4.
CXCL12 induces migration and invasion of HMVP2 cells. **A** and **B,** Cells in 12-well plates scratched with 200 μL pipette tips and treated with vehicle control, CXCL12 (100 ng/mL), IL6 (10 ng/mL), AMD3100 (40 μg/mL), or CXCL12 + AMD3100 at 0 and 18 hours posttreatment. Quantitation of migration levels is presented as mean ± SEM of three independent experiments. ***, $P < 0.001$; (one-way ANOVA). **C** and **D,** NMVP and HMVP2 cells were seeded in Matrigel in the upper transwell chambers and then placed into 24-well plates with medium that contained the vehicle (control), CXCL12 (100 ng/mL), IL6 (10 ng/mL), AMD3100 (40 μg/mL), or CXCL12 + AMD3100. After 18 hours, the invading cells in the lower chamber were fixed, stained, and visualized by light microscopy. Quantitation of invading cells presented as mean ± SEM of three independent experiments. ***, $P < 0.001$; (one-way ANOVA).

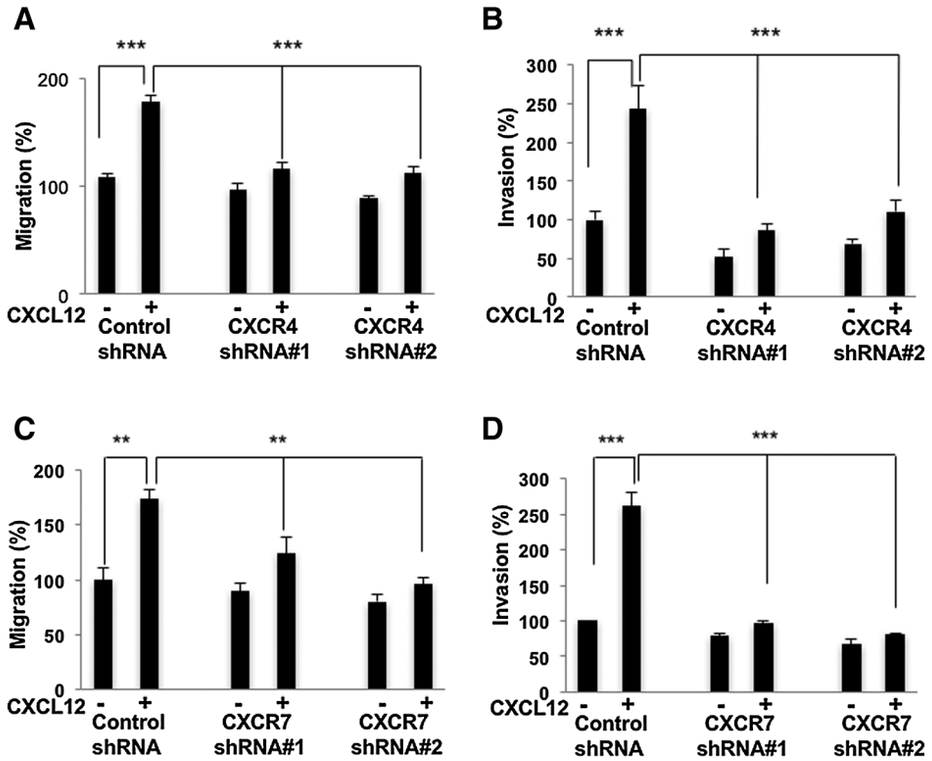

Figure 5.
CXCR4 and CXCR7 knockdown decreases migration and invasion in HMVP2 cells. Cells [transfected with control or CXCR4 shRNA (**A**); transfected with control or CXCR7 shRNA (**C**)] in 12-well plates scratched with 200 μL pipette tips and treated with vehicle control or CXCL12 (100 ng/mL). Quantitation of migration levels were presented as mean ± SEM of three independent experiments. **, $P < 0.01$; ***, $P < 0.001$; (Student *t* test). Cells [transfected with control or CXCR4 shRNA (**B**); transfected with control or CXCR7 shRNA (**D**)] were seeded in Matrigel in the upper transwell chambers and then placed into 24-well plates with medium that contained the vehicle (control) or CXCL12 (100 ng/mL). After 18 hours, the invading cells in the lower chamber were fixed, stained, and visualized by light microscopy. Quantitation of invading cells are presented as mean ± SEM of three independent experiments. ***, $P < 0.001$; (Student *t* test).

CXCL12 induces cancer-associated signaling pathways in HMVP2 cells

Previous reports indicate that binding of CXCL12 to its receptor(s) activates various cell signaling pathways, such as PI3K/AKT, ERK, and JNK pathways (24, 27). As shown in Fig. 6, CXCL12 treatment of HMVP2 cells led to activation of signaling pathways, including AKT, STAT3, NFκB, and MAPKs (both JNK and ERK), as assessed by the phosphorylation status of these proteins over a 30-minute time course. We also examined the effect of CXCL12 on these signaling pathways in NMVP cells. Treatment of cells with CXCL12 led to a rapid (15 minutes) activation of multiple signaling pathways in HMVP2 cells but not NMVP cells (Fig. 6A and B). This is consistent with lower CXCR4 and CXCR7 expression level in NMVP and supports the hypothesis that the activation of these signaling events is mediated through CXCR4 and CXCR7. The involvement of CXCR4 was further confirmed in HMVP2 cells pretreated with AMD3100, which led to significantly decreased activation of STAT3, NFκB, ERK, and JNK signaling (see Supplementary Fig. S6).

Finally, we used CXCR4 and CXCR7 knockdown HMVP2 cells to measure CXCL12-induced signaling. As shown in Supplementary Fig. S7, treatment with CXCL12 led to activation of STAT3, NFκB, and JNK in control shRNA-expressing cells similar to the parental HMVP2 cells. However, cells with CXCR4 knockdown showed lower activation of these signaling pathways upon treatment with CXCL12. Similarly, knockdown of CXCR7 also led to decreased activation of these signaling pathways upon stimulation with CXCL12 (Supplementary Fig. S8).

Discussion

Obesity is a risk factor for higher grade and more aggressive prostate cancer, and a number of mechanisms have been proposed to account for this observation (47). Recent attention has turned to ppWAT as a source of locally produced factors that may drive tumor progression (48). Furthermore, evidence from our laboratories has revealed that ASCs, the perivascular mesenchymal stem cells, serve as adipocyte progenitors in the WAT and represent a cell population that may be of particular importance to the obesity–cancer link (49). In mouse models, ASCs have been shown to infiltrate tumors and promote cancer progression by increasing vascularization and stimulating malignant cell survival and proliferation (50–52). Our recent report provides evidence that in obese prostate cancer patients, ASCs are guided to tumors by chemokines, CXCL1 and CXCL8 (20). Here, by using both *in vivo* and *in vitro* models, we show that the SVF of ppWAT is a rich source of growth factors, cytokines, and chemokines that are produced at high levels in obese mice. The role of CXCL12–CXCR4 axis in progression of various cancers, including prostate cancer, is well documented (28–31). However, the cell source of CXCL12 has remained unclear and whether this chemokine gradient contributes to cancer-promoting effects of obesity has remained a subject of debate.

Here, we provide evidence that ASC-derived CXCL12 signaling via CXCR4 and CXCR7 in malignant epithelial cells contributes to prostate cancer progression in obese HiMyc mice. As we recently reported, the DIO regimen significantly increased, whereas 30% CR significantly reduced the incidence and progression rate of locally invasive adenocarcinoma in HiMyc mice (33). As shown

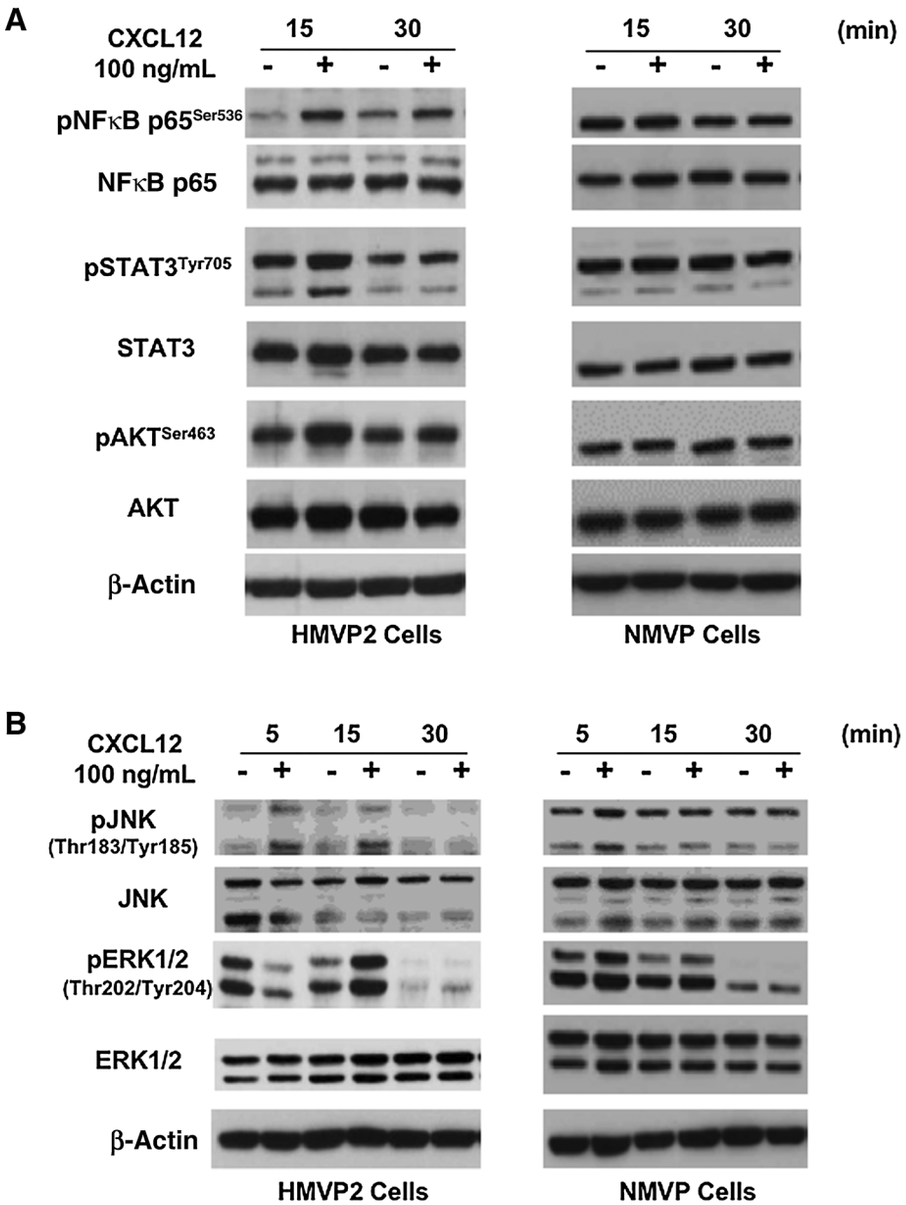

Figure 6.
Activation of NFκB, STAT3, and MAPK signaling by CXCL12 in HMVP2 cells. **A** and **B,** Protein lysates were prepared from cultured NMVP and HMVP2 cells treated with CXCL12 (100 ng/mL) for 5 to 30 minutes and subjected to Western blot analysis using antibodies for the indicated phospho and total proteins. Relative protein levels were quantitated by densitometry; β-actin was used to control for protein loading. Representative blots of three separate experiments with similar results are shown.

in Fig. 1, increased adiposity in HiMyc mice led to infiltration of adipocytes and inflammatory cells (T lymphocyte and macrophages) into the stromal compartment of the prostate tumors that develop in the VP of these mice. In previous studies, we also showed that there was a dramatic increase in both macrophages and T cells in the stromal compartment of these tumors consistent with the current results (33). Analysis of the SVF from ppWAT of obese HiMyc mice revealed dramatic upregulation (mRNA) of various chemokines (including CXCL12 and its receptors CXCR4 and CXCR7), cytokines, growth factors, and other signaling molecules known to be involved in cancer and cancer progression. Furthermore, immunofluorescence staining confirmed high levels of CXCL12 protein in the stromal compartment of the VP of obese HiMyc mice and high protein expression of CXCR4 and CXCR7 in the epithelial compartment of the tumors. Thus, obesity dramatically affected the tumor microenvironment, supporting the hypothesis that these changes contributed to the observed effects on tumor progression (33).

CXCL12 and its receptors have been described in a variety of solid tumors and tumor cells, including breast, lung, prostate, and pancreatic cancers (reviewed in ref. 24), are strongly linked to prostate cancer bone metastasis, and have been shown to be markers for poor prognosis (53, 54). By using cultured mouse ASCs, we found that these cells do express high mRNA levels of CXCL12 relative to HMVP2 prostate cancer tumor cells, indicating that the dramatically increased expression of CXCL12 in the SVF of obese HiMyc mice might be contributed by the ASCs that are present. It is also possible that other cells in the ppWAT, including macrophages and neutrophils (55), may contribute to the increase in CXCL12, as well as a number of other molecules that

were found to be upregulated, and this remains to be fully explored. Nevertheless, we believe that the ASCs are an important source of CXCL12 and other chemokines, especially in the obese state that can drive tumor progression and represent a potential target for therapeutic interventions. The current results support the hypotheses that upregulation of CXCL12 in either the ppWAT, the tumor stromal compartment, or both as well as upregulation of CXCR4 and CXCR7 in the prostate cancer epithelial cells contribute to the effects of obesity on prostate cancer progression in HiMyc mice. These data also suggest the possibility that differences in levels of CXCR4 and CXCR7 in subpopulations of tumor cells may provide selectivity in response to CXCL12 in driving tumor progression. HMVP2 cells represent a tumor-initiating cell line with stem/progenitor properties as described previously (40). As shown in Fig. 3, these cells expressed relatively high levels of CXCR4 and CXCR7 compared with NMVP and HMVP1 cells. In further support of this hypothesis, Dubrovska and colleagues reported that in human prostate cancer cell lines (DU145 and PC3), CXCR4 expression was elevated in the $CD44^+/CD133^+$ subpopulation of cells and that these cells were considerably more tumorigenic (56), and recent evidence suggests that CXCR7 is involved in maintaining the stem-like properties of breast, glioblastoma, and lung cancer cells (57–59).

Using HMVP2 prostate cancer cells, we found that CXCL12 significantly simulated their migration and invasion but did not produce similar effects on normal (immortalized) prostate epithelial cells (NMVP cells) derived from the VP of wild-type (FVB/N) mice. IL6, a cytokine whose mRNA was also found to be highly upregulated in the SVF of ppWAT from obese HiMyc mice, did not induce migration or invasion of HMVP2 cells. These effects of CXCL12 correlated with the levels of CXCR4 and CXCR7 protein detected in the cells and with selective activation of several key signaling pathways, such as NFκB, STAT3, and MAPKs. Furthermore, blocking CXCR4 or CXCR7 either genetically or pharmacologically abrogated the effect of CXCL12 on migration, invasion, and signal transduction. Collectively, these data further support the hypothesis that differences in levels of CXCR4 and CXCR7 in subpopulations of tumor cells may provide selectivity in response to CXCL12 in driving tumor progression.

The results presented here demonstrate that obesity-induced prostate cancer progression in HiMyc mice is mediated, at least in part, via the CXCL12–CXCR4/CXCR7 signaling axis. Although these data confirm the importance of CXCL12 signaling, other factors are likely involved in obesity-driven prostate cancer progression. Indeed, a number of other molecules were significantly upregulated in the SVF of ppWAT (Supplementary Fig. S1). Previously, other chemokines including CCL5, CCL7, CXCL1, CXCL8, CXCL16, and their receptors CCR3, CXCR1, CXCR2, and CXCR6, have been implicated in prostate cancer progression (20, 21, 23). In a recent report, Laurent and colleagues showed that periprostatic adipocytes secrete higher CCL7 in obesity and that this chemokine stimulates the invasion of CCR3-expressing tumor cells (21). This suggests that in obesity, CXCL12 may work together with other chemokines and adipokines to promote prostate cancer aggressiveness. Finally, recent studies indicate that NF-κB activation in mesenchymal progenitors (such as ASCs) "licenses" them to execute their immunosuppressive properties, which could contribute to tumor immune evasion and increased progression (60, 61). Therefore, other mechanisms may also contribute to enhanced tumor progression in obesity such as altered immunosurveillance.

In conclusion, the current data suggest that targeting the CXCL12–CXCR4/CXCR7 signaling axis may be a potential strategy for offsetting the effects of obesity on prostate cancer progression. We demonstrate that ASCs are an important source of CXCL12 in the ppWAT as well as the tumor stroma. Several recent reports (50, 52, 62) identify ASCs as a potential target for therapeutic interventions that could simultaneously inactivate numerous signaling processes induced by these cells in the tumor microenvironment. Future studies will explore the possibility of using these approaches in combination with conventional cancer therapies.

Disclosure of Potential Conflicts of Interest

No potential conflicts of interest were disclosed.

Authors' Contributions

Conception and design: A. Saha, M.G. Kolonin, J. DiGiovanni
Development of methodology: A. Saha, F. Su, J. DiGiovanni
Acquisition of data (provided animals, acquired and managed patients, provided facilities, etc.): A. Saha, S. Ahn, F. Su, J. DiGiovanni
Analysis and interpretation of data (e.g., statistical analysis, biostatistics, computational analysis): A. Saha, S. Ahn, J. Blando, F. Su, M.G. Kolonin, J. DiGiovanni
Writing, review, and/or revision of the manuscript: A. Saha, S. Ahn, J. Blando, F. Su, J. DiGiovanni
Administrative, technical, or material support (i.e., reporting or organizing data, constructing databases): M.G. Kolonin, J. DiGiovanni
Study supervision: A. Saha, J. DiGiovanni

Grant Support

This study was supported by NIH grant R01 CA196259 to J. DiGiovanni and M. G. Kolonin and Start-up funds to J. DiGiovanni from the University of Texas at Austin.

The costs of publication of this article were defrayed in part by the payment of page charges. This article must therefore be hereby marked *advertisement* in accordance with 18 U.S.C. Section 1734 solely to indicate this fact.

Received January 27, 2017; revised June 7, 2017; accepted July 3, 2017; published OnlineFirst July 7, 2017.

References

1. Nomura AM. Body size and prostate cancer. Epidemiol Rev 2001;23:126–31.
2. Porter MP, Stanford JL. Obesity and the risk of prostate cancer. Prostate 2005;62:316–21.
3. Flavin R, Zadra G, Loda M. Metabolic alterations and targeted therapies in prostate cancer. J Pathol 2011;223:283–94.
4. Allott EH, Masko EM, Freedland SJ. Obesity and prostate cancer: weighing the evidence. Eur Urol 2013;63:800–9.
5. Spitz MR, Strom SS, Yamamura Y, Troncoso P, Babaian RJ, Scardino PT, et al. Epidemiologic determinants of clinically relevant prostate cancer. Int J Cancer 2000;89:259–64.
6. Graham S, Haughey B, Marshall J, Priore R, Byers T, Rzepka T, et al. Diet in the epidemiology of carcinoma of the prostate gland. J Natl Cancer Inst 1983;70:687–92.
7. Strom SS, Yamamura Y, Forman MR, Pettaway CA, Barrera SL, DiGiovanni J. Saturated fat intake predicts biochemical failure after prostatectomy. Int J Cancer 2008;122:2581–5.
8. Kondo Y, Homma Y, Aso Y, Kakizoe T. Promotional effect of two-generation exposure to a high-fat diet on prostate carcinogenesis in ACI/Seg rats. Cancer Res 1994;54:6129–32.
9. Eheman C, Henley SJ, Ballard-Barbash R, Jacobs EJ, Schymura MJ, Noone AM, et al. Annual Report to the Nation on the status of cancer, 1975–2008,

featuring cancers associated with excess weight and lack of sufficient physical activity. Cancer 2012;118:2338–66.
10. De Nunzio C, Albisinni S, Freedland SJ, Miano L, Cindolo L, Finazzi Agro E, et al. Abdominal obesity as risk factor for prostate cancer diagnosis and high grade disease: a prospective multicenter Italian cohort study. Urol Oncol 2013;31:997–1002.
11. van Kruijsdijk RC, van der Wall E, Visseren FL. Obesity and cancer: the role of dysfunctional adipose tissue. Cancer Epidemiol Biomarkers Prev 2009;18:2569–78.
12. Coussens LM, Werb Z. Inflammation and cancer. Nature 2002;420:860–7.
13. Park J, Euhus DM, Scherer PE. Paracrine and endocrine effects of adipose tissue on cancer development and progression. Endocr Rev 2011;32: 550–70.
14. Trayhurn P, Wood IS. Adipokines: inflammation and the pleiotropic role of white adipose tissue. Br J Nutr 2004;92:347–55.
15. Ouchi N, Parker JL, Lugus JJ, Walsh K. Adipokines in inflammation and metabolic disease. Nat Rev Immunol 2011;11:85–97.
16. Khandekar MJ, Cohen P, Spiegelman BM. Molecular mechanisms of cancer development in obesity. Nat Rev Cancer 2011;11:886–95.
17. Roberts DL, Dive C, Renehan AG. Biological mechanisms linking obesity and cancer risk: new perspectives. Annu Rev Med 2010;61:301–16.
18. Ribeiro RJ, Monteiro CP, Cunha VF, Azevedo AS, Oliveira MJ, Monteiro R, et al. Tumor cell-educated periprostatic adipose tissue acquires an aggressive cancer-promoting secretory profile. Cell Physiol Biochem 2012;29: 233–40.
19. van Roermund JG, Hinnen KA, Tolman CJ, Bol GH, Witjes JA, Bosch JL, et al. Periprostatic fat correlates with tumour aggressiveness in prostate cancer patients. BJU Int 2011;107:1775–9.
20. Zhang T, Tseng C, Zhang Y, Sirin O, Corn PG, Li-Ning-Tapia EM, et al. CXCL1 mediates obesity-associated adipose stromal cell trafficking and function in the tumour microenvironment. Nat Commun 2016; 7:11674.
21. Laurent V, Guerard A, Mazerolles C, Le Gonidec S, Toulet A, Nieto L, et al. Periprostatic adipocytes act as a driving force for prostate cancer progression in obesity. Nat Commun 2016;7:10230.
22. Sun X, Cheng G, Hao M, Zheng J, Zhou X, Zhang J, et al. CXCL12/CXCR4/CXCR7 chemokine axis and cancer progression. Cancer Metastasis Rev 2010;29:709–22.
23. Balkwill F. Cancer and the chemokine network. Nat Rev Cancer 2004;4: 540–50.
24. Hattermann K, Mentlein R. An infernal trio: the chemokine CXCL12 and its receptors CXCR4 and CXCR7 in tumor biology. Ann Anat 2013;195: 103–10.
25. Aiuti A, Webb IJ, Bleul C, Springer T, Gutierrez-Ramos JC. The chemokine SDF-1 is a chemoattractant for human CD34+ hematopoietic progenitor cells and provides a new mechanism to explain the mobilization of CD34+ progenitors to peripheral blood. J Exp Med 1997;185:111–20.
26. Yin Q, Jin P, Liu X, Wei H, Lin X, Chi C, et al. SDF-1alpha inhibits hypoxia and serum deprivation-induced apoptosis in mesenchymal stem cells through PI3K/Akt and ERK1/2 signaling pathways. Mol Biol Rep 2011;38:9–16.
27. Domanska UM, Kruizinga RC, Nagengast WB, Timmer-Bosscha H, Huls G, de Vries EG, et al. A review on CXCR4/CXCL12 axis in oncology: no place to hide. Eur J Cancer 2013;49:219–30.
28. Sakao K, Vyas AR, Chinni SR, Amjad AI, Parikh R, Singh SV. CXCR4 is a novel target of cancer chemopreventative isothiocyanates in prostate cancer cells. Cancer Prev Res (Phila) 2015;8:365–74.
29. Singh S, Singh UP, Grizzle WE, Lillard JW Jr. CXCL12-CXCR4 interactions modulate prostate cancer cell migration, metalloproteinase expression and invasion. Lab Invest 2004;84:1666–76.
30. Conley-LaComb MK, Saliganan A, Kandagatla P, Chen YQ, Cher ML, Chinni SR. PTEN loss mediated Akt activation promotes prostate tumor growth and metastasis via CXCL12/CXCR4 signaling. Mol Cancer 2013;12:85.
31. Dirat B, Ader I, Golzio M, Massa F, Mettouchi A, Laurent K, et al. Inhibition of the GTPase Rac1 mediates the antimigratory effects of metformin in prostate cancer cells. Mol Cancer Ther 2015;14:586–96.
32. Domanska UM, Timmer-Bosscha H, Nagengast WB, Oude Munnink TH, Kruizinga RC, Ananias HJ, et al. CXCR4 inhibition with AMD3100 sensitizes prostate cancer to docetaxel chemotherapy. Neoplasia 2012; 14:709–18.
33. Blando J, Moore T, Hursting S, Jiang G, Saha A, Beltran L, et al. Dietary energy balance modulates prostate cancer progression in Hi-Myc mice. Cancer Prev Res (Phila) 2011;4:2002–14.
34. Ellwood-Yen K, Graeber TG, Wongvipat J, Iruela-Arispe ML, Zhang J, Matusik R, et al. Myc-driven murine prostate cancer shares molecular features with human prostate tumors. Cancer Cell 2003;4:223–38.
35. Nesbit CE, Tersak JM, Prochownik EV. MYC oncogenes and human neoplastic disease. Oncogene 1999;18:3004–16.
36. Hawksworth D, Ravindranath L, Chen Y, Furusato B, Sesterhenn IA, McLeod DG, et al. Overexpression of C-MYC oncogene in prostate cancer predicts biochemical recurrence. Prostate Cancer Prostatic Dis 2010;13: 311–5.
37. Jenkins RB, Qian J, Lieber MM, Bostwick DG. Detection of c-myc oncogene amplification and chromosomal anomalies in metastatic prostatic carcinoma by fluorescence in situ hybridization. Cancer Res 1997;57: 524–31.
38. Sato K, Qian J, Slezak JM, Lieber MM, Bostwick DG, Bergstralh EJ, et al. Clinical significance of alterations of chromosome 8 in high-grade, advanced, nonmetastatic prostate carcinoma. J Natl Cancer Inst 1999;91:1574–80.
39. Gurel B, Iwata T, Koh CM, Jenkins RB, Lan F, Van Dang C, et al. Nuclear MYC protein overexpression is an early alteration in human prostate carcinogenesis. Mod Pathol 2008;21:1156–67.
40. Saha A, Blando J, Fernandez I, Kiguchi K, DiGiovanni J. Linneg Sca-1high CD49fhigh prostate cancer cells derived from the Hi-Myc mouse model are tumor-initiating cells with basal-epithelial characteristics and differentiation potential in vitro and in vivo. Oncotarget 2016;7: 25194–207.
41. Saha A, Blando J, Tremmel L, DiGiovanni J. Effect of metformin, rapamycin and their combination on growth and progression of prostate tumors in HiMyc mice. Cancer Prev Res 2015;8:597–606.
42. Liang CC, Park AY, Guan JL. In vitro scratch assay: a convenient and inexpensive method for analysis of cell migration in vitro. Nat Protoc 2007;2:329–33.
43. Valster A, Tran NL, Nakada M, Berens ME, Chan AY, Symons M. Cell migration and invasion assays. Methods 2005;37:208–15.
44. Sirin O, Kolonin MG. Treatment of obesity as a potential complementary approach to cancer therapy. Drug Discov Today 2013;18:567–73.
45. Nakao N, Nakayama T, Yahata T, Muguruma Y, Saito S, Miyata Y, et al. Adipose tissue-derived mesenchymal stem cells facilitate hematopoiesis *in vitro* and *in vivo*: advantages over bone marrow-derived mesenchymal stem cells. Am J Pathol 2010;177:547–54.
46. Jung Y, Kim JK, Shiozawa Y, Wang J, Mishra A, Joseph J, et al. Recruitment of mesenchymal stem cells into prostate tumours promotes metastasis. Nat Commun 2013;4:1795.
47. Blando J, Saha A, Kigichi K, DiGiovanni J. Obesity, inflammation and prostate cancer. In: Dannenberg AJ, Berger NA, editors. Obesity, inflammation and cancer, energy balance and cancer. New York: Springer; 2013.
48. Finley DS, Calvert VS, Inokuchi J, Lau A, Narula N, Petricoin EF, et al. Periprostatic adipose tissue as a modulator of prostate cancer aggressiveness. J Urol 2009;182:1621–7.
49. Zhang Y, Daquinag A, Traktuev DO, Amaya-Manzanares F, Simmons PJ, March KL, et al. White adipose tissue cells are recruited by experimental tumors and promote cancer progression in mouse models. Cancer Res 2009;69:5259–66.
50. Daquinag AC, Tseng C, Zhang Y, Amaya-Manzanares F, Florez F, Dadbin A, et al. Targeted proapoptotic peptides depleting adipose stromal cells inhibit tumor growth. Mol Ther 2016;24:34–40.
51. Zhang Y, Daquinag AC, Amaya-Manzanares F, Sirin O, Tseng C, Kolonin MG. Stromal progenitor cells from endogenous adipose tissue contribute to pericytes and adipocytes that populate the tumor microenvironment. Cancer Res 2012;72:5198–208.
52. Klopp AH, Zhang Y, Solley T, Amaya-Manzanares F, Marini F, Andreeff M, et al. Omental adipose tissue-derived stromal cells promote vascularization and growth of endometrial tumors. Clin Cancer Res 2012;18:771–82.
53. Akashi T, Koizumi K, Tsuneyama K, Saiki I, Takano Y, Fuse H. Chemokine receptor CXCR4 expression and prognosis in patients with metastatic prostate cancer. Cancer Sci 2008;99:539–42.
54. Mochizuki H, Matsubara A, Teishima J, Mutaguchi K, Yasumoto H, Dahiya R, et al. Interaction of ligand-receptor system between stromal-cell-derived factor-1 and CXC chemokine receptor 4 in human prostate cancer: a

possible predictor of metastasis. Biochem Biophys Res Commun 2004; 320:656–63.
55. Hausman DB, DiGirolamo M, Bartness TJ, Hausman GJ, Martin RJ. The biology of white adipocyte proliferation. Obes Rev 2001;2:239–54.
56. Dubrovska A, Elliott J, Salamone RJ, Telegeev GD, Stakhovsky AE, Schepotin IB, et al. CXCR4 expression in prostate cancer progenitor cells. PLoS One 2012;7:e31226.
57. Tang X, Li X, Li Z, Liu Y, Yao L, Song S, et al. Downregulation of CXCR7 inhibits proliferative capacity and stem cell-like properties in breast cancer stem cells. Tumour Biol 2016;37:13425–33.
58. Wu YC, Tang SJ, Sun GH, Sun KH. CXCR7 mediates TGFbeta1-promoted EMT and tumor-initiating features in lung cancer. Oncogene 2016;35: 2123–32.
59. Walters MJ, Ebsworth K, Berahovich RD, Penfold ME, Liu SC, Al Omran R, et al. Inhibition of CXCR7 extends survival following irradiation of brain tumours in mice and rats. Br J Cancer 2014;110:1179–88.
60. English K. Mechanisms of mesenchymal stromal cell immunomodulation. Immunol Cell Biol 2013;91:19–26.
61. Choi H, Lee RH, Bazhanov N, Oh JY, Prockop DJ. Anti-inflammatory protein TSG-6 secreted by activated MSCs attenuates zymosan-induced mouse peritonitis by decreasing TLR2/NF-kappaB signaling in resident macrophages. Blood 2011;118:330–8.
62. Nowicka A, Marini FC, Solley TN, Elizondo PB, Zhang Y, Sharp HJ, et al. Human omental-derived adipose stem cells increase ovarian cancer proliferation, migration, and chemoresistance. PLoS One 2013;8: e81859.